学位申請論文

足立公夫

論 文 内 容 の 要 旨

報告番号	乙第　　号	氏名	足立公夫
論文調査担当者	主査　広田　　裏 辻川郁二　　山本常信		

（論文題目）

ESR Study of Quasi-One-Dimensional Ising-Like Antiferromagnet $CsCoCl_3$

（擬1次元Ising-like型反強磁性体$CsCoCl_3$の電子スピン共鳴の研究）

（論文内容の要旨）

擬1次元磁性体において、低温で短距離秩序が発達した状態は、磁気鎖中のスピン配列の局所的乱れを磁壁と見なした時、その非線形波動が、連続体近似の下で、sine-Gordon方程式で記述され、磁気ソリトンとして注目されている。しかし実験的に磁気ソリトンの研究された例は少く、実験的研究の発展が望まれている。磁壁が極端に薄くなった場合に相当する、$S=1/2$を持つIsingに近い系のスピンダイナミックスは、熱的に励起された磁壁が鎖中を伝播するモデルで記述出来、一種のソリトンと見なし得る。申請者は電子スピン共鳴（ESR）の手段により、1次元Ising-like型反強磁性体の典型である$CsCoCl_3$について、電子スピン共鳴（ESR）の手段を用いて実験を行い、得られた結果を伝播磁壁によるESR信号であるとして解析し、理論的に予測されるものと良い一致を得ている。

実験は単結晶試料でXバンドのESR装置を用いて液体He温度以上で行

ESR Study of Quasi-One-Dimensional Ising-Like Antiferromagnet $CsCoCl_3$

Kimio ADACHI

Department of Chemistry, Faculty of Science,

Kyoto University, Kyoto 606

Electron spin resonance was measured at 9.40 GHz as a function of temperature in a quasi-one-dimensional Ising-like antiferromagnet $CsCoCl_3$. Observed resonance in the partially disordered phase, $T_{N2} \lesssim T < T_{N1}$ and its neighborhood is interpreted in terms of ESR due to spins at propagating domain walls in one-dimensional Ising-like antiferromagnet. The theory developed by Shiba and the present author gives a more consistent interpretation of the temperature dependence of the absorption intensity and the angular dependences of the resonance field and the linewidth than the existing theories. Discussion is given in connection with spin-cluster resonance.

§1. Introduction

In recent years, there has been a growing interest in the elementary magnetic excitations and their dynamics in one-dimensional Ising-like systems [1-2] Especially, much attention is devoted to one-dimensional Ising-like antiferromagnet (hereafter, abbreviated as 1D I-L [AF]) in connection with propagating domain walls (solitons) predicted by Villain.[1] Experimentally, the central peak of inelastic neutron diffraction characteristic of the propagating domain walls was found in $CsCoCl_3$ by Yoshizawa et al..[3]

ESR is also expected to be a useful technique for the study of the propagating domain walls A theoretical study on the ESR due to spins at propagating domain walls in 1D I-L [AF] was developed by Shiba and the present author [4] Comparison with the theory and experiments is of interest.

ESR in 1D I-L system is, however, closely related to spin-cluster resonance (SCR)[5] associated with a pair of domain walls. SCR has been observed in 1D I-L [AF] compounds[6,7] as well as in 1D I-L [F] compounds.[5,8-10] In $CsCoCl_3$, ESR due to the propagating domain walls and/or the spin-cluster excitations are expected to be observed.

The magnetic properties of $CsCoCl_3$ are well known from the measurements of magnetic susceptibility,[11] specific heat,[12,13] neutron diffraction[14,15] and ^{133}Cs- and ^{59}Co-NMR.[16,17] Magnetic excitations and their dynamics have been also studied by experiments of inelastic neutron scattering,[3,18-21] far infrared excitation[22-24] and ^{133}Cs-NMR.[16] Ishimura and Shiba[25] calculated transverse and longitudinal magnetic responses in $CsCoCl_3$ and gave a new interpretation of the spin wave spectrum different from des Cloizeaux and Gaudin's

theory [26] The experiment by Satija et al.[27] confirmed their prediction.

$CsCoCl_3$ has a flattened simple hexagonal lattice of magnetic ions with fictitious spin S=1/2 at low temperatures. One-dimensional magnetic chains extend along the c-axis Owing to the triangular lattice in the c-plane, a characteristic magnetic phase transition occurs at $T_{N2} \simeq 9$ K. One third of magnetic chains loses its long range coherence in the c-plane above the temperature. This partially disordered phase is stable up to the Néel temperature $T_{N1} \simeq 21$ K. Mekata[28] interpreted the phase transition on the basis of molecular field theory of two-dimensional triangular lattice. By taking into account of the interchain interaction as a staggered molecular field, Shiba[29] extended the model to the three-dimensional lattice. Based on the theory, he gave a satisfactory interpretation of magnon Raman spectra[22-24] in $CsCoCl_3$ in terms of discrete odd-number-magnon excitations.

The present paper reports the results of ESR in a typical S=1/2 1D I-L [AF], $CsCoCl_3$. We show that the observed spectra are successfully explained in terms of the resonance due to spins at propagating domain walls Discussion in connection with SCR is also given.

§2. Experimental

Single crystals of $CsCoCl_3$ were grown from an equimolar mixture of CsCl and $CoCl_2$ in a quartz ampoule by the Bridgman method. Cleaving the crystals, samples with a suitable size for ESR measurement were prepared. Size effect of sample was not appreciable.

ESR spectra were collected in the temperature range 4.2 ∿ 77.3 K by a reflection type spectrometer with a TE_{011} rectangular cavity

operated at 9.40 GHz with an 80 Hz magnetic field modulation. As a g-marker DPPH powder was used. The sample temperature was controlled by regulating a heater and was measured with a calibrated germanium thermometer. Temperature was stabilized within 0.05 K.

§3. Results

When the temperature is raised from 4.2 K, a faint signal is found above 6 K at an external field of 1.26 kOe applied along the c-axis (the chain direction) The signal gets more intensity as temperature is increased and the peak-to-peak height attains its maximum at about 12 K. In the neighborhood of the temperature, the linewidth begins to increase considerably Above 17 K, the signal becomes undetectable again due to the line broadening. Throughout the temperature range, the resonance field remains constant within the experimental errors. The observed spectra are shown in Fig. 1.

Figure 2 shows the temperature dependence of the peak-to-peak height I_{pp} and peak-to-peak linewidth ΔH_{pp}. The absorption intensity was evaluated by the relation $I \propto I_{pp} \times \Delta H_{pp}^{2}$ which is reasonable for Gaussian as well as Lorentzian lineshapes. The absorption intensity in logarithmic scale is shown in Fig. 3 as a function of temperature. The observed intensity increases with increasing temperature and an anomaly in its temperature dependence is found in the vicinity of T_{N2}.

Figure 4 shows the angular dependences of the resonance field and the linewidth in the a-c plane at 11.9 K. As the direction of the applied field is rotated from the c-axis (parallel to the chain) to the a-axis (perpendicular to the chain), the resonance field shifts to the higher field side and the linewidth is broadened.

At liquid helium temperatures, an extremely weak and slightly sample dependent signal was observed. It may be attributed to paramagnetic impurity judging from its temperature dependence[30]; it decreases with increasing temperature. We are not concerned with this signal in this paper because it is out of our present interest.

§4. Interpretation in terms of ESR due to propagating domain walls

The observed ESR has entirely different temperature dependences of the resonance field as well as the absorption intensity from those of antiferromagnetic resonance due to collective spin motions. Paramagnetic impurity ions yield also a quite different temperature dependence of absorption intensity from the observed one.[30] In the following, we apply the theory of ESR due to propagating domain walls to interprete the present experimental results. As will be seen, the theory affords a more consistent interpretation of the results than SCR model.

§4.1 Theory

In this section, the theory of ESR due to propagating domain walls is summarized briefly. The detailed description is appeared in a separate paper [4]

The model Hamiltonian for S=1/2 1D I-L [AF] in a magnetic field is given

$$\mathcal{H} = 2J \Sigma_i [S_i^z S_{i+1}^z + \varepsilon (S_i^x S_{i+1}^x + S_i^y S_{i+1}^y)] - \mu_B H \Sigma_i (g_{//} \cos\theta S_i^z + g_\perp \sin\theta S_i^y) \quad (1)$$

$$\equiv \mathcal{H}_0 + \mathcal{H}_z ,$$

where $J > 0$, $\varepsilon << 1$ and θ is the angle between z-axis and the external

magnetic field. We define ψ_j as the state in which a single domain wall located between j and j+1 sites in an infinite chain. Using a linear combination of the functions $\Psi = \Sigma_j c_j \psi_j$, $\mathcal{H}$ can be diagonalized. Then, we obtain the eigenvalues

$$\lambda_{\pm} = J(1 + 2\varepsilon\cos(2ka)) \pm \sqrt{(g_{\perp}\mu_B H\sin\theta \cos(ka))^2 + (\tfrac{1}{2}g_{//}\mu_B H\cos\theta)^2} \tag{2}$$

which gives the dispersion relations of the propagating domain walls and the corresponding eigenfunctions $\Psi_{\pm}(k)$ can be obtained. An oscillating field $H'e^{i\omega t}$ along y direction perpendicular to z-x plane induces an energy absorbing transition from the state $\Psi_-(k)$ to the state $\Psi_+(k)$ By evaluating its transition probability, the ESR absorption intensity $I(\omega)$ is obtained as follows;

$$I(\omega) \propto \frac{\mathrm{Im}\,\chi^{yy}(\omega)}{(g_{\perp}\mu_B)^2 N} = \frac{1}{2Z}\,\beta\,\frac{\omega^2}{\omega_2^2 - \omega_1^2}\sqrt{\frac{\omega^2 - \omega_1^2}{\omega_2^2 - \omega^2}}$$

$$\times e^{-\beta J}\; e^{-\beta 2\varepsilon J(2\omega^2 - \omega_1^2 - \omega_2^2)/(\omega_2^2 - \omega_1^2)},$$

$$(\omega_1 < \omega < \omega_2) \tag{3}$$

where $\beta = \frac{1}{kT}$, $Z = \frac{1}{N}\,\Sigma_k\, e^{-2\beta\varepsilon J\cos(2ka)}$ and

$$\begin{cases} \omega_1^2 = (g_{//}\mu_B H\cos\theta)^2 , \\ \omega_2^2 = (g_{//}\mu_B H\cos\theta)^2 + (2g_{\perp}\mu_B H\sin\theta)^2. \end{cases}$$

§4.2 Comparison with the theory

§4.2-1 Resonance field

For the external magnetic field along z-axis, the Eq.(3)

diverges at $\omega_2 = g_{//} \mu_B H$. If we assign the signal to the resonance at ω_2, $g_{//}$ is found to be $\simeq 5.33$. The value is close to $g_{//} \simeq 5.2 \pm 0.4$[22] or 4.8[24] deduced from the field dependence of the Raman spectrum. Since Eq. (3) is derived for an isolated chain, those resonant spins are considered to be free from the molecular field due to the neighboring chains. Actually in the magnetic structures of $CsCoCl_3$, a considerable number of chains are not subject to the molecular field due to interchain interaction as listed in Table I.

4.2-2 Temperature dependence of absorption intensity

From Eq. (3), the temperature dependence of the intensity for H// z-axis (chain direction) is found to be proportional to $\exp(-\beta J)$ at very low temperatures $kT \ll 2\beta J$ and $\beta \exp(-\beta J)$ at moderately low temperatures $2\varepsilon J \ll kT \ll J$ The difference comes from the fact that the domain walls with $ka \simeq \pi/2$ are more important at very low temperatures. The solid and dashed curves in Fig 3 show the relations $I \propto \beta \exp(-\beta J)$ and $I \propto \exp(-\beta J)$ with $J = 75$ K[18,19], respectively. The curves are normalized at 15 K for $T > T_{N2}$ and at T_{N2} for $T \lesssim T_{N2}$ because the chains with zero interchain molecular field have different weights in the two magnetic phases as given in Table I. When we use $\varepsilon \simeq 0.13$[27,29] and $J = 75$ K, the observed temperature region lies in $kT \sim 2\varepsilon J$ The present data show better agreement with theoretical prediction $\beta \exp(-\beta J)$ for moderately low temperatures.

In the low temperature phase, the weight of chains with zero molecular field is 1.6 times as large as that in the partial disordered phase. But the observed ratio of intensities in the two phases which corresponds to the ratio of weights is = 2.7 in good agreement with $\simeq 3.0$ deduced from recent Raman scattering [24] The disagreement of

the weight ratio between the theory and the experiment together with the gradual change of intensity at T_{N2} may be related to the second neighbor interaction and the effect of disordered chains.

§ 4.2-3 Angular dependence of resonance field

Since Im $\chi^{YY}(\omega)$ in Eq. (3) diverges at ω_2, the observed resonance field should be close to ω_2 Then, the angular dependence of the resonance field is expressed as

$$H_{obs}(\theta) = g_{//} H_0 / \sqrt{(g_{//}\cos\theta)^2 + (2g_{\perp}\sin\theta)^2}, \qquad (5)$$

where H_0 denotes the resonance field for the magnetic field along the c-axis. Substituting $g_{//} = 5.33$ and $g_{\perp} = 1.77$, the solid curve in Fig.4 is obtained in good agreement with the experimental values.

§ 4.2-4 Line shape

The line shape given by Eq. (3) is a δ-function peak at ω_2 for $\theta = 0°$. For $\theta \neq 0°$, it has, however, an unusual asymmetry with a divergence at the high-frequency edge ω_2 and has a discernible shoulder at low-frequency side, especially in the very low temperature region, $kT << 2\varepsilon J$ The following features may be related to the predicted line shape: The higher field-tail of the spectrum increases with θ especially at low temperatures and the line is broadened remarkably at $\theta = 90°$ The ratio of the peak-to-peak linewidth at $\theta = 0°$ and $\theta = 90°$ amounts to almost ≈5,while dipolar broadening gives at most the ratio of 2. The contribution from the components lower than ω_2 to resonance gives an account of the remarkable broadening.

§5. Analysis based on SCR

In the preceding section, it is shown that the experimental

data can be interpreted satisfactorily in terms of ESR due to propagating domain walls. But we cannot exclude a priori another possible resonance SCR associated with a pair of domain walls In this section an analysis based on Shiba's theory[29] is given.

For the evaluation of the eigenenergies of the spin-cluster excitations, the Hamiltonian should include an interchain interaction term $\mathcal{H}'$ in addition to the terms in Eq. (1) as

$$\mathcal{H} = \mathcal{H}_0 + \mathcal{H}' + \mathcal{H}_z \tag{6}$$

Below T_{N1}, the second term may be expressed in terms of the staggered molecular field h_j due to interchain interaction as

$$\mathcal{H}' = - \Sigma_j h_j S_j^z = - \Sigma_j (-1)^j \cdot h \; S_j^z \quad (h \geq 0) \tag{7}$$

In the case of purely one-dimensional lattice or h = 0, the excited state levels form a continuum arround 2J, while they are split into discrete levels in finite h. The excited states with $S^z = \pm 1$ are degenerate as far as the external magnetic field H is zero. The degeneracy is lifted in finite H. On the other hand, the excited states with $S^z = 0$ remain doubly degenerate even in finite H. The so-called Ising basis functions for $S^z = \pm 1$ are given by

$$\begin{cases} \Psi_1(k) = \sqrt{2/N} \; \Sigma_j \, e^{ikR_j} \, S_j^{\pm} \, \Psi_{N1} \, , \\ \Psi_3(k) = \sqrt{2/N} \; \Sigma_j \, e^{ikR_j} \, S_j^{\pm} \, S_{j+1}^{\mp} \, S_{j+2}^{\pm} \, \Psi_{N1} \, , \\ \quad . \quad . \quad . \quad . \quad . \\ \Psi_{N-1}(k) = \sqrt{2/N} \; \Sigma_j \, e^{ikR_j} \, S_j^{\pm} \prod_{\nu=1}^{(\frac{N}{2})-1} (\, S_{j+2\nu-1}^{\mp} \, S_{j+2\nu}^{\pm} \,) \, \Psi_{N1} \, , \end{cases} \tag{8}$$

where Ψ_{N1} stands for one of the two Néel states. These functions describe the states with a pair of domain walls. For the longitudinal

field, using these functions the matrix elements of the excited states with $S^z = \pm 1$ are given apart from the common diagonal element ($= - N\{\frac{1}{2} J(1+\varepsilon^2) + \frac{h}{2}\}$) by

$$\langle \Psi_{2\nu-1}(k) | \mathcal{H} | \Psi_{2\nu'-1}(k) \rangle$$

$$= \begin{cases} 2J\left(1 + \frac{3}{2}\varepsilon^2 - \frac{1}{2}\varepsilon^2 \delta_{\nu,1} \right) + (2\nu-1)h \mp g_{//}\mu_B H & \text{for } \nu'=\nu \\ V_1 & \text{for } \nu' = \nu+1 \\ V_1^* & \text{for } \nu' = \nu-1 \\ V_2 & \text{for } \nu' = \nu+2 \\ V_2^* & \text{for } \nu' = \nu-2 \\ 0 & \text{otherwise} \end{cases} , \qquad (9)$$

where $V_1 = \varepsilon J(1 + e^{-2ika})$ and $V_2 = - \frac{1}{2}\varepsilon^2 J(1+ e^{-4ika})$ Similarly. the even-number-magnon bound states with $S^z = 0$ are obtained as

$$\langle \Psi_{2\nu}(k) | \mathcal{H} | \Psi_{2\nu'}(k) \rangle$$

$$= \begin{cases} 2J\left(1 + \frac{3}{2}\varepsilon^2 - \frac{1}{4}\varepsilon^2 \delta_{\nu,1} \right) + 2\nu h & \text{for } \nu' =\nu \\ \text{the same as in Eq (9)} & \text{otherwise,} \end{cases} \qquad (10)$$

where $\Psi_{2\nu}$ are defined as

$$\begin{cases} \Psi_2(k) = \sqrt{2/N} \ \Sigma_j \ e^{ikR_j} \ S_j^- \ S_{j+1}^+ \ \Psi_{N1} \ , \\ \Psi_4(k) = \sqrt{2/N} \ \Sigma_j \ e^{ikR_j} \ \prod_{\nu=0}^{1} \ (\ S_{j+2\nu}^- \ S_{j+2\nu+1}^+ \ ) \ \Psi_{N1} \\ \cdots \quad \cdot \ \cdot \end{cases} \qquad (11)$$

The above expressions include up to second order terms of ε because the relevant energies are comparable with them. Since the states with different S^z do not mix with each other, the eigenenergies of the system can be calculated by respective diagonalizations of Eqs. (9) and (10) We evaluated the eigenenergies for $h=2J'$, $h=4J'$ and $h=6J'$ as a function of H, using the values; J=75 K, ε=0.13, g =5 33 and $J'=0.96\times10^{-2}$J.[29]

Taking into consideration of the selection rule, the resonance absorptions are expected to be observed at 3.00. 5 53 (h=2J'), 7.25, 9.78 (h=4J') and 11.5, 14 0 (h=6J'] in kOe. No signal is detected at these fields within the sensitivity of the spectrometer

The intensity of SCR associated with domain walls which are subject to the effective molecular field (h≠0) varies with temperature as exp(-2βJ) in 1D Ising antiferromagnet.[4] The expected temperature dependence for the case shown by a dotted line in Fig. 3 agrees by no means with the experimental results.

In order to obtain the angular dependence of the resonance field, we must solve simultaneously Eqs. (9) and (10) after converting $g_{//}\mu_B H$ by $g_{//}\mu_B H\cos\theta$ and taking into account of the off-diagonal element $-\frac{1}{2} g_{\perp}\mu_B H\sin\theta$ The results for h=2J' are shown in Fig. 5. As the off-diagonal elements are relatively small compared with other terms, the angular dependence obeys the $1/\cos\theta$ law,

$$H_{obs} = H_0/\cos\theta \qquad (12)$$

also in this case as in 1D Ising systems.[6-9] It is,however, not the present case.

6. Discussion

It is concluded from the analyses in the foregoing two sections that the observed resonance does not come from the spin-cluster excitations but from the propagating domain walls. To the author's knowledge, this is the first observation of ESR due to the propagating domain walls. A spin-cluster excitation is associated with a pair of domain walls, while a single domain wall takes part in a propagating domain wall. Since the excess energy per wall is J, the probabilities of thermally activated single domain wall and spin-clusters are roughly exp(-βJ) and

$\exp(-2\beta J)$, respectively. The higher probability of the thermally activated single domain walls may be the reason why we could observe the resonance due to the propagating domain walls rather than the SCR.

The temperatures of measurements are neither $T<<2\varepsilon J/k$ nor $T>>2\varepsilon J/k$ but $T\simeq 2\varepsilon J/k$. The temperature dependence $\beta\exp(-\beta J)$ which is valid in $T>>2\varepsilon J/k$ gives better fitting to the experimental values than $\exp(-\beta J)$ for $T<< 2\varepsilon J/k$. It is, however, difficult to predict exactly the temperature dependence in this intermediate temperature region.

ESR of Co^{2+} ions dissolved dilutely in $CsMgCl_3$ gives the values $g_{//}=7.2$[11] and 7 37[31] and $g_{\perp}=2.51$.[31] The $g_{//}$ values are considerably higher than the present value $g_{//}=5.33$. Euler and Garrett[32] calculated $g_{//}$ value of Co^{2+} ion in $CsCoCl_3$ and obtained 7 63. But the ground state of Co^{2+} ion is sensitive to the surroundings since the orbital angular momentum is not completely quenched. The $g_{//}$ value may be different from in concentrated and dilute systems.

Acknowledgment

The author would like to express his grateful acknowledgment to Professor M. Mekata and Dr. Y. Ajiro for valuable discussions. He is also very much indebted to Professor H. Shiba and Professor K. Hirakawa of University of Tokyo and Professor M. Date of Osaka University for helpful discussions.

References

1) J Villain: Physica 79B (1975) 1.

2) M. Fowler and M. W. Puga: Phys. Rev. B18 (1978) 421.

3) H. Yoshizawa, K. Hirakawa, S.K. Satija and G. Shirane: Phys. Rev. B23 (1981) 2298.

4) H. Shiba and K. Adachi: J Phys Soc. Jpn. 51 (1981)

5) M. Date and M. Motokawa: Phys. Rev Lett. 16 (1966) 1111.

6) A. Herwijer, W.J.M. de Jonge, A.C. Botterman, A.L.M. Bongaarts and J.A. Cowen: Phys Rev. B5 (1972) 4618.

7) Q.A.G. van Vlimmeren and W.L.M. de Jonge: Phys. Rev. B19 (1979) 1003.

8) M. Date and M. Motokawa: J Phys Soc. Jpn. 24 (1968) 41.

9) Y. Ajiro and S. Matsukawa: Phys. Lett. 72A (1979) 367

10) Y Ajiro, K. Adachi and T Sharyo: J Phys. Soc. Jpn. 50 (1981) 1.

11) N. Achiwa: J Phys. Soc. Jpn. 27 (1969) 561.

12) K. Iio, H. Hyodo and K. Nagata: private communication.

13) K. Adachi, Y. Ajiro and M. Mekata: in preparation.

14) H. Melamud, H. Pinto, J. Makovsky and H. Shaked: Phys. Status Solidi (b) 63 (1974) 699.

15) M. Mekata and K. Adachi: J. Phys. Soc. Jpn. 44 (1978) 806.

16) K. Adachi, M. Hamashima, Y Ajiro and M. Mekata: J. Phys. Soc. Jpn. 47 (1979) 780.

17) T. Kubo, K. Adachi, M. Mekata and A. Hirai: Solid State Commun. 28 (1979) 553.

18) U. Tellenbach: J Phys. C11 (1978) 2287

19) H. Yoshizawa and K. Hirakawa: J Phys. Soc. Jpn. 46 (1979) 448.

20) K. Hirakawa and H. Yoshizawa: J Phys. Soc. Jpn. 46 (1979) 455.

21) W.J.L. Buyers, J Yamanaka, S.E. Nagler and R.L. Armstrong: Solid State Commun. 33 (1980) 857

22) W. Breitling, W. Lehmann, T.P. Srinivasan, R. Weber and U. Dürr: Solid State Commun. 24 (1977) 267

23) W. Breitling, W. Lehmann and R. Weber: J Magn. Magn. Mat. 10 (1979) 25

24) W. Lehmann, W. Breitling and R. Weber: to be published in J. Phys. C.

25) N. Ishimura and H. Shiba: Prog. Theor Phys. 63 (1980) 743.

26) J des Cloizeaux and M. Gaudin: J Math. Phys. 7 (1966) 1384.

27) S.K. Satija, G. Shirane, H. Yoshizawa and K. Hirakawa: Phys. Rev. Lett. 44 (1980) 1548.

28) M. Mekata: J Phys. Soc. Jpn. 42 (1977) 76.

29) H. Shiba: Prog. Theor. Phys. 64 (1980) 466.

30) N. Fujii, M. Motokawa and M. Date: J. Phys. Soc. Jpn. 25 (1968) 700.

31) H. Rinneberg and H. Hartmann: J Chem. Phys. 52 (1970) 5814.

32) N.B. Euler and B.B. Garrett: J. Phys. Chem. Solids. 42 (1981) 7.

Figure captions

Fig 1. The resonance spectra at various temperatures. Magnetic field is applied along the c-axis.

Fig. 2. Temperature dependence of peak-to-peak height I_{pp} and peak-to-peak linewidth ΔH_{pp}. Lines are aid to eye only.

Fig. 3. Temperature dependence of absorption intensity Solid, dashed and dotted lines represent $\beta\exp(-\beta J)$, $\exp(-\beta J)$ and $\exp(-2\beta J)$ dependences with J=75 K, respectively.

Fig 4 Angular dependences of resonance field and linewidth at 11.9 K. Solid line is calculated by Eq. (5) for $g_{//}$ =5.33 and $g_{\perp}$ =1.77 Dashed line is aid to eye only.

Fig 5. Angular dependence of the lowest resonance field with h=2J'

Table I The molecular fields due to interchain interaction and their probability weights in the two magnetic phases of $CsCoCl_3$.[29]

phase	molecular field h	weight
fully ordered phase	6J′	$\frac{1}{3}$
$T<T_{N2}$	0	$\frac{2}{3}$
partially disordered phase	6J′	$\frac{1}{8}\times\frac{2}{3}=\frac{1}{12}$
	4J′	$\frac{3}{8}\times\frac{2}{3}=\frac{1}{4}$
$T_{N2}<T<T_{N1}$	2J′	$\frac{3}{8}\times\frac{2}{3}=\frac{1}{4}$
	0	$\frac{1}{3}+\frac{1}{12}=\frac{5}{12}$

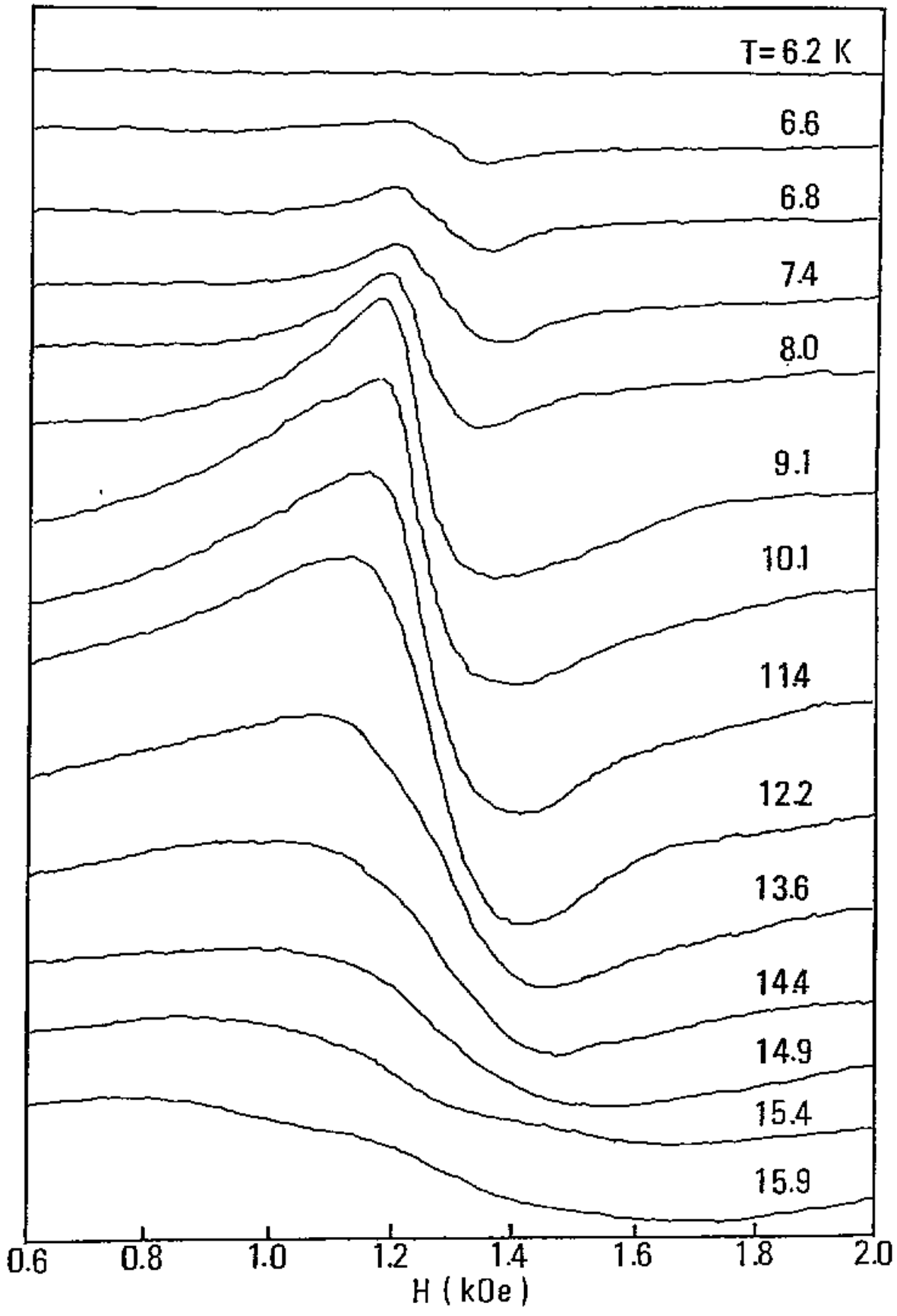
T= 6.2 K
6.6
6.8
7.4
8.0
9.1
10.1
11.4
12.2
13.6
14.4
14.9
15.4
15.9
0.6
0.8
1.0
1.2
1.4
1.6
1.8
2.0
H (kOe)

FIG. 1

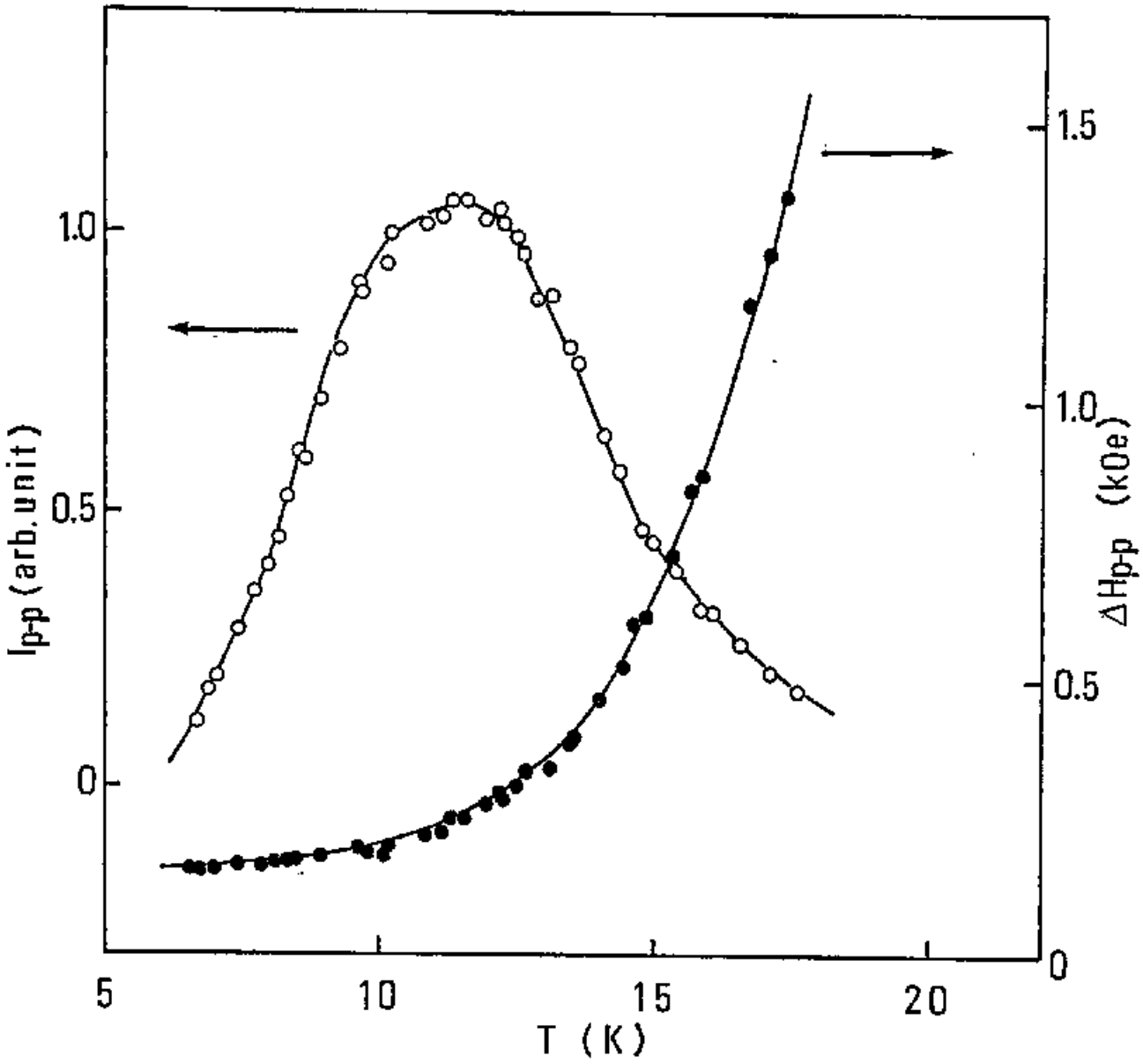
1.0
0.5
0
$I_{p\text{-}p}$ (arb. unit)
1.5
1.0
0.5
0
$\Delta H_{p\text{-}p}$ (kOe)
5
10
15
20
T (K)

FIG. 2

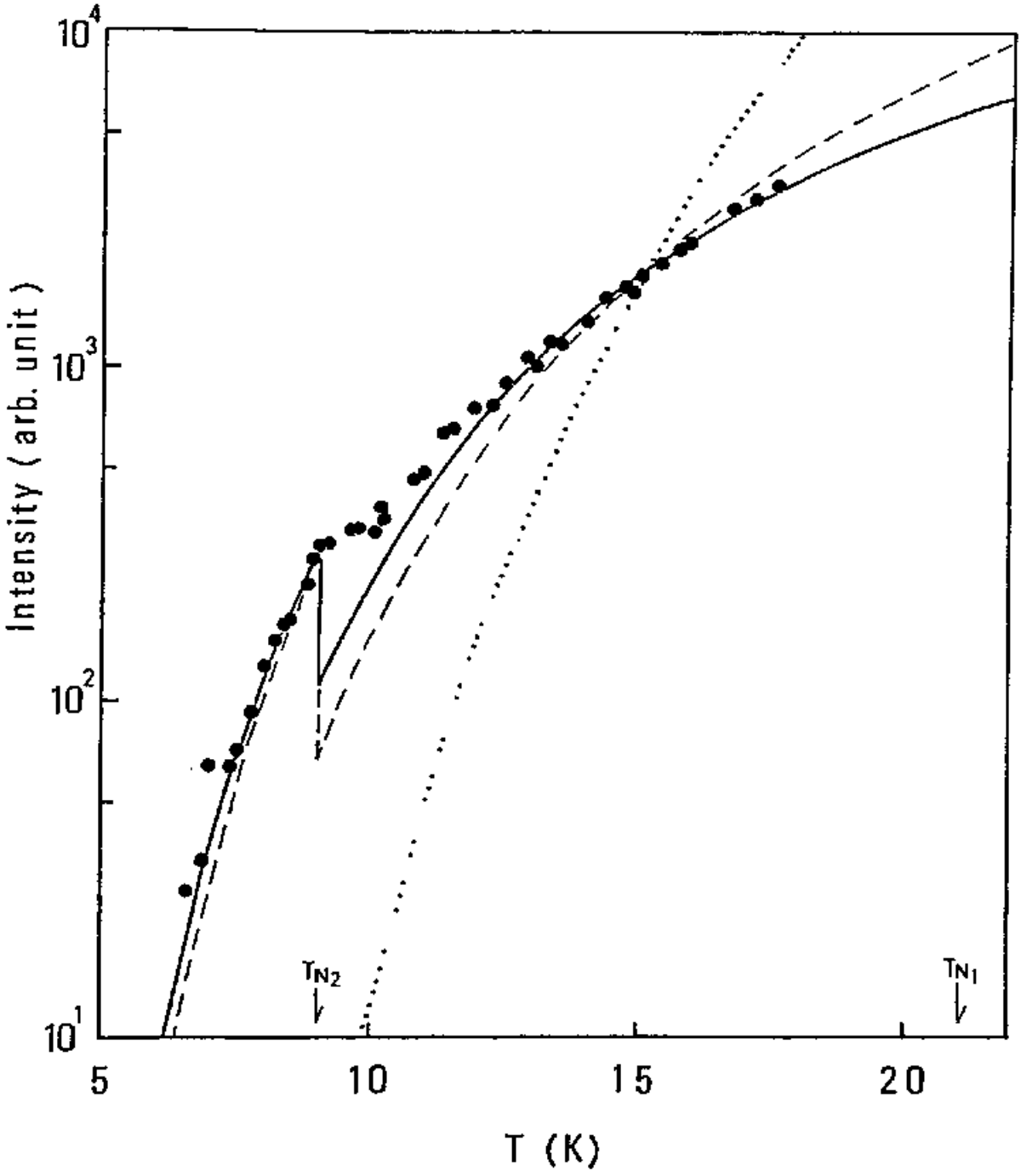

FIG. 3

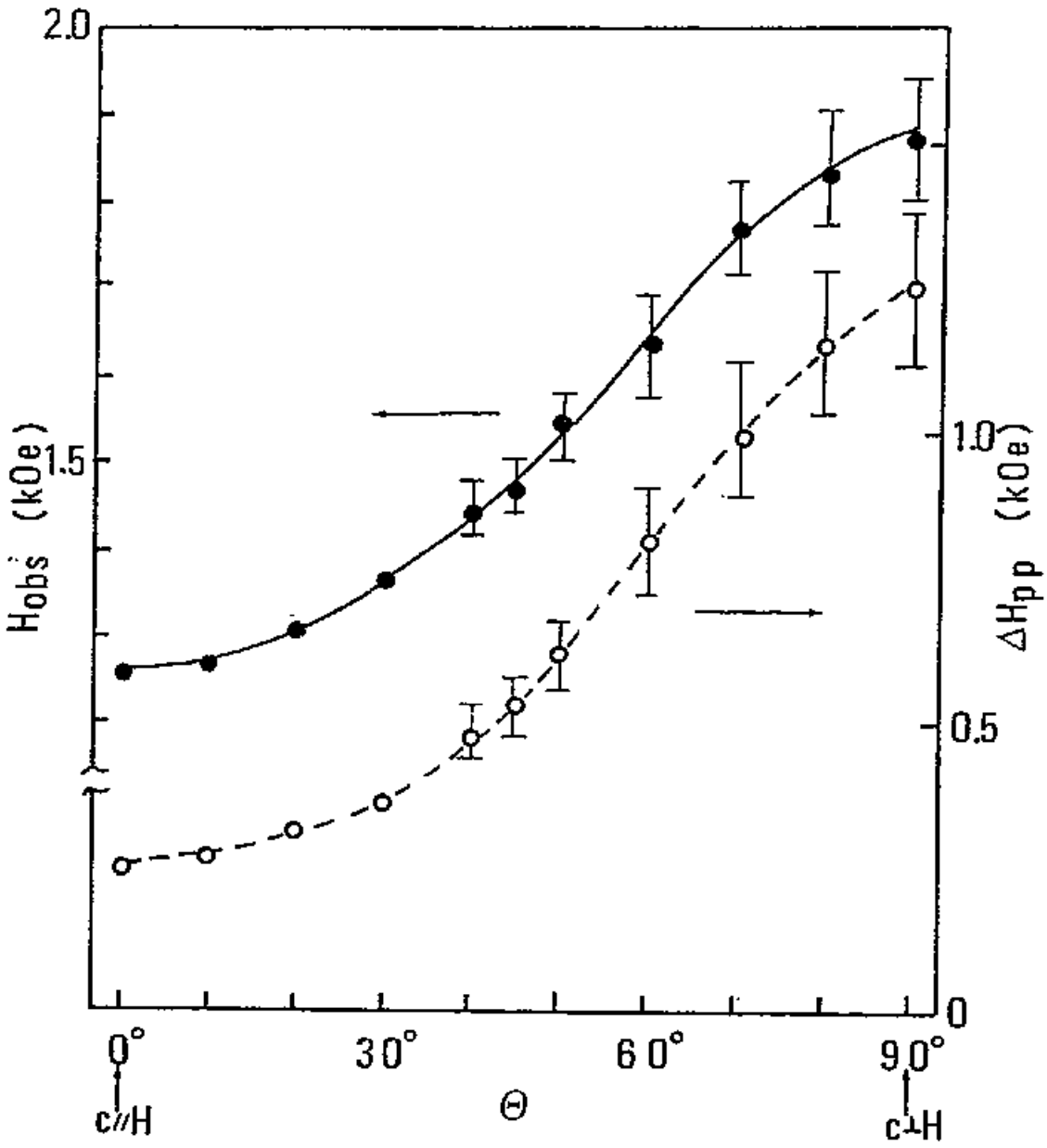

FIG. 4

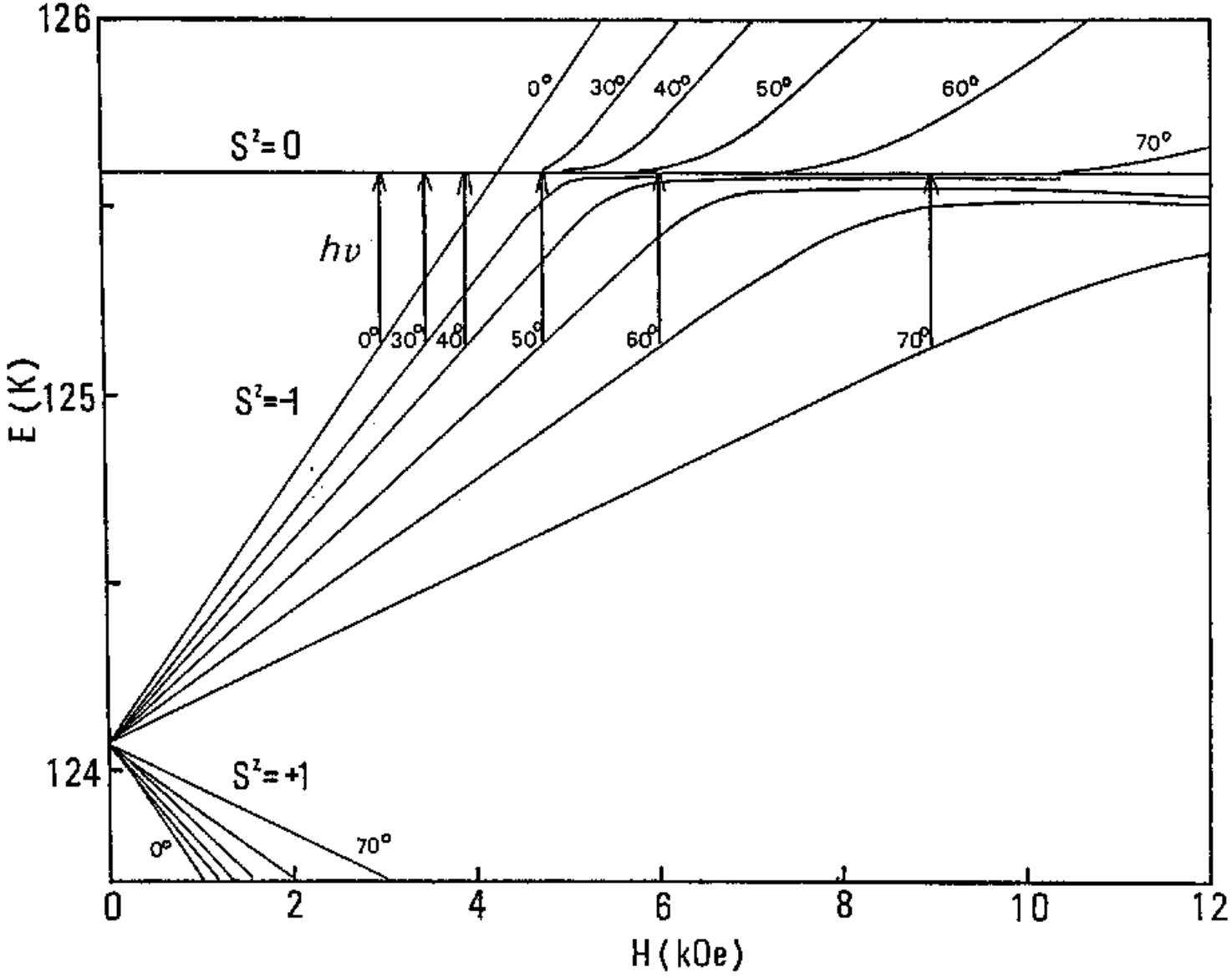

FIG. 5